Mechanics of semiflexible chains formed by poly(ethylene glycol)-linked paramagnetic particles

Sibani Lisa Biswal
Department of Chemical Engineering, Stanford University, Stanford, California 94305, USA

Alice P. Gast*
Department of Chemical Engineering, MIT, Cambridge, Massachusetts 02139, USA

(Received 31 January 2003; published 7 August 2003)

Magnetorheological particles, permanently linked into chains, provide a magnetically actuated means to manipulate microscopic fluid flow. Paramagnetic colloidal particles form reversible chains by acquiring dipole moments in the presence of an external magnetic field. By chemically connecting paramagnetic colloidal particles, flexible magnetoresponsive chains can be created. We link the paramagnetic microspheres using streptavidin-biotin binding. Streptavidin coated microspheres are placed in a flow cell and a magnetic field is applied, causing the particles to form chains. Then a solution of polymeric linkers of bis-biotin-poly(ethylene glycol) molecules is added in the presence of the field. These linked chains remain responsive to a magnetic field; however, in the absence of an external magnetic field these chains bend and flex due to thermal motion. The chain flexibility is determined by the length of the spacer molecule between particles and is quantified by the flexural rigidity or bending stiffness. To understand the mechanical properties of the chains, we use a variety of optical trapping experiments to measure the flexural rigidity. Increasing the length of the poly(ethylene glycol) chain in the linker increases the flexibility of the chains.

DOI: 10.1103/PhysRevE.68.021402 PACS number(s): 82.70.Dd

I. INTRODUCTION

Magnetorheological fluids are suspensions of paramagnetic colloidal particles, which aggregate into chains when subjected to an external magnetic field. In the absence of an external magnetic field, the particles remain randomly distributed. Linking these particles together while under a magnetic field creates stable permanently linked magnetoresponsive chains. The chains stiffen and align in a magnetic field; when the magnetic field is removed, the chains fluctuate and randomly orient due to thermal motion.

Paramagnetic particles are already commonly used in the separation of biopolymers and cells [1]. Additionally, there has been a growing interest for using paramagnetic particles to manipulate microscopic fluid flow [2,3]. The advantage of paramagnetic particles is their ability to interact dynamically with fluids and be actuated by an external field that does not interfere with other microfluidic processes. Another unique feature is that the surface of the particles may be functionalized. One of the disadvantages in using paramagnetic particles is that a continual magnetic field is needed to create and control a structure. In this work we bind paramagnetic particles together to form linked chains which act as dynamic structures in both the presence and the absence of an external magnetic field.

There are a variety of linking chemistries that can be used to create permanently linked chains of magnetic particles. In order to have a successful linker, a symmetric bifunctional molecule is needed to react with the complementary functional group on the paramagnetic particle. Previously, we had synthesized linked chains by forming covalent bonds between neighboring amine-functionalized microspheres with glutaraldehyde [4]. In this work, we link paramagnetic particles using the binding reaction between the protein streptavidin and the ligand biotin. Additionally, we explore the effects of the length of the bis-biotin agent on the chain flexibility.

Chains with controllable stiffness provide interesting microstructures having a field response that can be exploited in microfluidic devices. For this reason, we wish to characterize the mechanical properties of these chains in the field-off state. Optical traps have become a useful tool for studying the micromechanics of colloidal particles [5]. We present a number of experiments probing the static and dynamic response of individual chains to external forces produced by optical traps. Similar experiments have been performed for other elastic filaments such as actin and microtubules [6–8]. From these experiments, we characterize the chain shape and dynamic response with models developed for elastic beams and semiflexible polymers. Although we sometimes observe chains with defects, kinks, and pivot points, the chains studied here for the most part behave elastically with uniform bending stiffness along the length of the chain.

II. MATERIALS AND METHODS

A. Preparation of permanently linked paramagnetic chains

We create linked magnetoresponsive chains by using streptavidin-biotin binding chemistry to connect paramagnetic colloidal chains created in a magnetic field. Streptavidin is a tetrameric protein: it consists of four identical subunits, each of which has a biotin binding site for the ligand biotin. Though no covalent bonds are formed, the high affinity of biotin for streptavidin, $K_a = 10^{15}\ \mathrm{M}^{-1}$, is caused by van der Waals interactions and multiple dipolar and hydrogen bonding interactions in streptavidin's biotin binding pocket [9]. It is one of the strongest known biological inter-

*Electronic address: gast@mit.edu

actions between a protein and a ligand so that the resulting complexes can thought to be irreversibly bound [10].

We link the chains and perform all of the characterization experiments in a 50×50 mm^2 by 30 μm flow cell made from a bovine serum albumin (BSA) (Sigma Chemicals) coated glass microscope slide attached to a BSA-coated glass coverslip with double-stick tape. Coating the glass slides and coverslips with BSA prevents adsorption of the microspheres to the glass surface. We place a dilute (0.01% by volume) suspension of commercially available paramagnetic colloidal particles with covalently bound streptavidin (Seradyne Inc., Sera-Mag Part 3015-2105, 1 ml, 1% solids by weight) in a *p*H 7 borate buffer containing 1% Tween 20 (Sigma Chemicals) in the flow cell. The particles are made up of a carboxylate-modified polystyrene core to which a layer of magnetite is attached. This magnetic layer is encapsulated by an outer polymer surface, which provides carboxyl groups to covalently attached streptavidin with a biotin binding capacity of 5000 pmol/mg microsphere [11]. The paramagnetic polystyrene microspheres have a mean diameter of $2a=0.78$ μm, confirmed by transmission electron microscopy, and contain 40% (weight) monodomain iron oxide (magnetite) grains. Once the particles are placed in the flow cell, a magnetic field of approximately 30 mT with two neodymium-iron-boron magnets (McMaster-Carr Corporation) is applied. Within about 10 min in the field, the particles have aggregated into linear chains and a linking reaction proceeds.

To link particles, we react the protein streptavidin with polymers carrying the ligand biotin on both ends. Optimal biotin-binding capabilities can be obtained by using a biotin derivative that has an extended spacer arm, which reduces steric hindrance and provides a flexible linker. The bis-biotin-poly(ethylene glycol) (PEG) molecule is ideal because the PEG length can be adjusted to increase flexibility of the chain. We test two linkers: bis-biotin-PEG with MW=733 (Pierce Chemicals) and bis-biotin-PEG with MW=3400 (Shearwater Polymers), where MW stands for molecular weight. The linker is introduced at a concentration of 10 mg/ml in borate buffer, chosen so that an excess of biotin molecules ensures the saturation of the streptavidin molecules coating the paramagnetic particles. Chains are also linked with glutaraldehyde following a procedure developed previously [4].

The cell is then sealed with epoxy to prevent evaporation. The PEG 733 solution is placed in the flow cell for 6 h at room temperature while the PEG 3400 solution is placed in the flow cell for 12 h at 33° C. After this time, the field is turned off and chain properties are probed using optical tweezers. These chains remain stable in this cell for several weeks and can be recovered and preserved in buffer.

Figure 1 shows chains linked with PEG 733 randomly oriented due to thermal motion in the absence of an external magnetic field. As shown in Fig. 2(a), in the absence of an external magnetic field, the chains can bend and flex. Once an external magnetic field is applied to the system, the chains stiffen in the direction of the magnetic field as shown in Fig. 2(b).

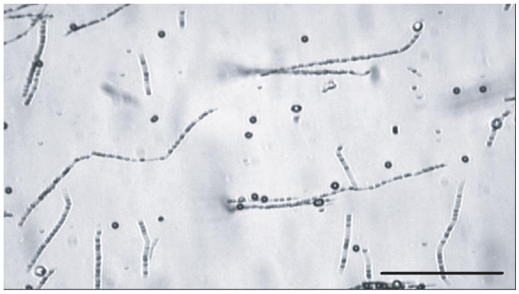

FIG. 1. Paramagnetic cross-linked chains in the absence of an external magnetic field. Particles are 0.86 μm in diameter. Larger particles seen are 3.36-μm polystyrene particles serving as tether handles for the optical traps. Scale bar: $=50$ μm.

We readily monitor the translation, rotation, and fluctuations during linking experiments through video microscopy. Qualitatively, chains linked with the PEG 3400 fluctuate much more than chains linked with the PEG 733, indicating that increasing the molecular weight of the PEG spacer molecule produces a more flexible chain. By contrast, the chains linked with glutaraldehyde are noticeably much stiffer than those made with PEG-biotin spacers.

B. Optical trapping experiments

The iron oxide grains embedded within each paramagnetic microsphere absorb and scatter light such that they are very difficult to trap optically. For this reason, we attach ''tether handles'' [12] onto the chains. Biotinylated polystyrene microspheres (Polysciences) with a mean diameter of 3.36 μm are added to the bead solution and incorporated into the magnetic bead chains.

Our dual-trap optical tweezers are formed from a 5-W Nd:YAG (where YAG stands for yttrium aluminum garnet)

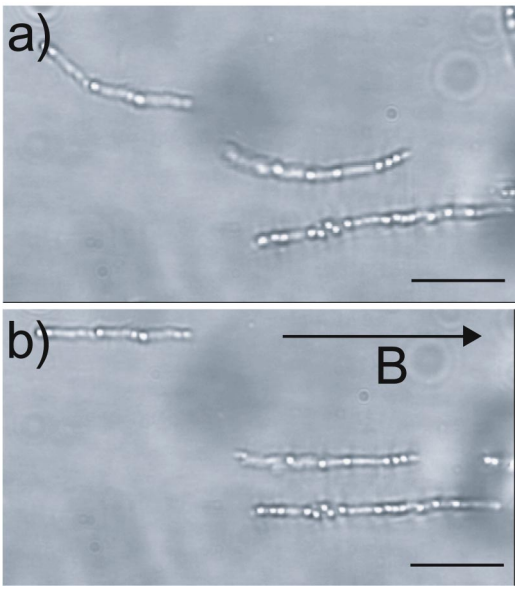

FIG. 2. (a) Cross-linked chains curve and flex without the presence of a magnetic field. (b) The chains stiffen in the direction of the external magnetic field strength of 31 mT. Scale bar: $=5$ μm.

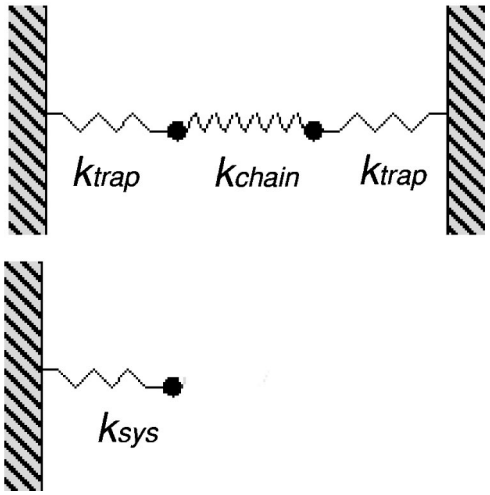

FIG. 3. The dual-trap chain system can be modeled as a system of connected springs. The traps have stiffness k_{trap} and the chain has stiffness k_{chain}. This system is equivalent to one fixed spring with system stiffness k_{sys}.

laser at a wavelength of 532 nm (Coherent). The beam is expanded and plane polarized as it passes through a polarizing cube splitter. The two beams are directed into a 63 $\times$/1.2 objective (Zeiss Plan-Neofluar) to create the optical traps. The laser beams are translated in two dimensions using Gimbal mirrors. The flow cell is translated relative to the optical traps with a motorized microscope stage (Newport) as described before [12].

Images are detected with a charge-coupled device camera (Hamamatsu) and continuously recorded with a super VHS video recorder (JVC). The video images were taken at 10 frames/s. and digitized using the public domain NIH software (Scion Image). The chain movements are measured from a binarized image; pixel coordinates for the centers of each particle are found with a modified NIH particle-tracking program macro.

We calibrate the stiffness of the optical trap, k_{trap}, using Stokes drag [13,14]. We hold a tether particle in an optical trap while translating the surrounding fluid at a constant velocity. From the drag force vs particle displacement, we determined that the trap stiffness k_{trap} is in the range of 50–100 pN/μm at a laser power of 40–100 mW. Our experiments take place where the optical traps have a maximum lateral trapping force of 55 pN. It is important to note that the chains can rotate inside the trap. We are able to monitor this rotation and analyze the chains independent of this rotational motion.

C. Elastic models

The optical traps attached to the ends of a chain can be modeled as a simple series of springs shown in Fig. 3. The tether handles are fixed to their positions with springs, each with trap stiffness k_{trap}. The chain connects the tethers and is represented by a spring with linkage stiffness k_{chain}. Following the model developed [13,15,16], this system is equivalent to a single tether connected to a fixed position by a spring with stiffness k_{sys}:

$$k_{sys}=\frac{k_{trap}k_{chain}}{k_{trap}+k_{chain}}+k_{trap}. \tag{1}$$

Linked chains undergo a variety of deformations depending on the applied force and the nature of the linker. When forces are applied along the length of the chain, it may either stretch or compress while forces applied transverse to the chain cause it to bend. We approximate the bending and stretching of these chains with models for elastic rods. The bending modulus of an elastic rod can be described in terms of the flexural rigidity, a length-independent measure of resistance to external bending forces. The bending energy per unit chain length, U, is related to the curvature as

$$U=\frac{EI}{2}\int_0^L\left(\frac{d\theta}{ds}\right)^2 ds, \tag{2}$$

where EI is the flexural rigidity, $d\theta/ds$ is the curvature, and s is the arclength along the chain. The flexural rigidity can be separated into the Young's modulus E and the moment of inertia, $I=\pi a^4/4$, for a rod with a circular cross section of radius a. The persistence length $L_p=EI/kT$ is directly proportional to the flexural rigidity.

The force required to stretch an elastic chain under small extensions will vary linearly with the change in length. The stiffness of the system, k_{sys}, can be converted into the system extension or Young's modulus by multiplying by the length of the chain, L, and dividing by the cross-sectional area A of the chain: $E=k_{sys}L/A$. By measuring the Young's modulus of the system and using Eq. (1), the stiffness of the chain, k_{chain}, can be determined providing a measure of the Young's modulus for the chains.

In the case of a chain that is parallel to the x axis undergoing small deflections, $s\approx x$, the curvature, $d\theta/ds$, can be linearized to d^2y/dx^2. The force per unit length, f, acting on a chain can be found by differentiating Eq. (2):

$$f=-EI\frac{d^4y}{dx^4}. \tag{3}$$

When a chain is being manipulated with optical tweezers, a single point force F_t is applied to the ends of the chain:

$$F_t=-EI\frac{d^3y}{dx^3}. \tag{4}$$

The reference frame chosen is for a chain that is fixed at one end; therefore, $y(0)=y'(0)=0$. While the other end is allowed to translate and rotate, implying that $y''(L)=0$. Inserting these boundary conditions into Eq. (4) gives the bent shape of the chain:

$$y(x)=\frac{F_tLx^2}{2EI}-\frac{F_tx^3}{6EI}. \tag{5}$$

1. Chain compression

When a compressive force is applied along the length of the chain, the chain deforms. This is similar to an elastic rod

undergoing an Euler buckling instability under externally imposed compressive forces [17–19]. We have used Euler's linearized equation of a rod under longitudinal compression to determine its shape. The chain shape can be analyzed by applying Euler's formula for one fixed end and the other free:

$$EI\frac{d^2\theta}{ds^2}=(-F_{||}+F_{\perp})\sin\theta, \tag{6}$$

where θ is the tangent angle along the chain, s is the arclength along the chain, and $F_{\parallel}$ and $F_{\perp}$ are the tangent and perpendicular components of the force acting on the end of the chain. Again, this equation can be linearized for small deflections:

$$EI\frac{d^2y}{dx^2}=-F_{||}y+F_{\perp}(L-x). \tag{7}$$

At the ends of the chains, the deflection is zero: $y(0)=y(L)=0$. Additionally, we analyze the shape of the compressed chain such that the end of the chain at the origin has $y'(0)=0$. Defining $k^2=F_{||}/EI$ in Eq. (7), the deflected shape of the chain due to a compressive force has a transcendental solution:

$$y(x)=\frac{F_{\perp}}{F_{||}k}[\sin kx-kL\cos kx+k(L-x)], \tag{8}$$

where the smallest nonzero value of k is determined by $\tan kL=kL=4.4934$. Note that the minimum force needed to bend the chain is $F_{cr}=2.04\pi^2EI/L^2$.

2. Chain relaxation

We can also measure the flexibility of a chain by observing its relaxation dynamics after deformation. Consider a chain that has been bent using optical tweezers. Once the end of the chain that has been translated is released from the optical trap, the chain straightens. By balancing the viscous drag force with the elastic forces acting upon the chain, the flexural rigidity can be determined from the change in the shape:

$$\zeta\frac{dy}{dt}=-EI\frac{d^4y}{dx^4}, \tag{9}$$

where ζ is the viscous drag coefficient. From slender-body hydrodynamics, a cylindrical body with an aspect ratio $a/L\gg 1$ has a drag coefficient [20]

$$\zeta=\frac{4\pi\eta}{\ln(L/a)+c}, \tag{10}$$

where η is the viscosity of the solution and c is a constant of order unity. Considering a chain fixed at one end and free at the other end, we get $y(0,t)=0$, $y'(0,t)=0$, and $y''(L,t)=0$, and $y'''(L,t)=0$. Following the solutions developed [17,21,22], the chain relaxation motion is given by

$$y(x,t)=\sum_k W_k(x)e^{-EIk^4t/\zeta}\int_0^L W_k(x)y(x,0)dx. \tag{11}$$

The bending modes are given by $d^4W(x)/dx^4=k^4/L^4$, where the general form of the transcendental solution can be written as

$$W_k=a_1\sin(kx/L)+a_2\cos(kx/L)+a_3\sinh(kx/L)+a_4\cosh(kx/L). \tag{12}$$

Applying the boundary conditions yields discrete values of k determined by $\cos k\cosh k=-1$; the smallest value of k is 1.875. The decay in the shape of the forced end of the chain is well approximated by the first bending mode:

$$\frac{y(L,t)}{y(L,0)}\sim e^{-C_1t}, \tag{13}$$

where

$$C_1=\frac{EIk^4}{\zeta L^4}. \tag{14}$$

III. RESULTS

We studied two biotinylated polymer spacers used to link the paramagnetic particles, PEG 733 and PEG 3400. Linking paramagnetic particles with the PEG 3400 was more difficult due to its higher molecular weight and relative dilution of biotinylated ends within the polymer coil. By increasing the time from 6 to 12 h and reaction temperature from room temperature to 33 deg, we are able to successfully link them; however, the increase in temperature increases the thermal motion of the chains, causing them to be corrugated. Chains made with the PEG 733 are much longer with average lengths ranging from 20–200 μm, while chains linked with PEG 3400 are 5–30 μm in length. In each optical trapping experiments, we study 5–12 chains varying in length from 20–50 μm; the mean flexural rigidity value is reported with a standard deviation.

A. Stretching experiments

We measured the force needed to extend the chain from its relaxed configuration. We perform stretching experiments on several chains linked with PEG 733 and PEG 3400, with our dual-trap tweezers. Each image of the chain is analyzed to determine the chain length as a function of the applied force. The plot shown in Fig. 4 is typical of these results; after an initial extension, the force versus extension plot is linear and the coefficient of extension is the slope. The initial extension is due to the tether deflection and rotation within the optical trap. The coefficient of extension can be converted into the stretching, or Young's modulus, by dividing by the cross-sectional area A of the chain:

$$\frac{F}{\Delta x/L}=EA. \tag{15}$$

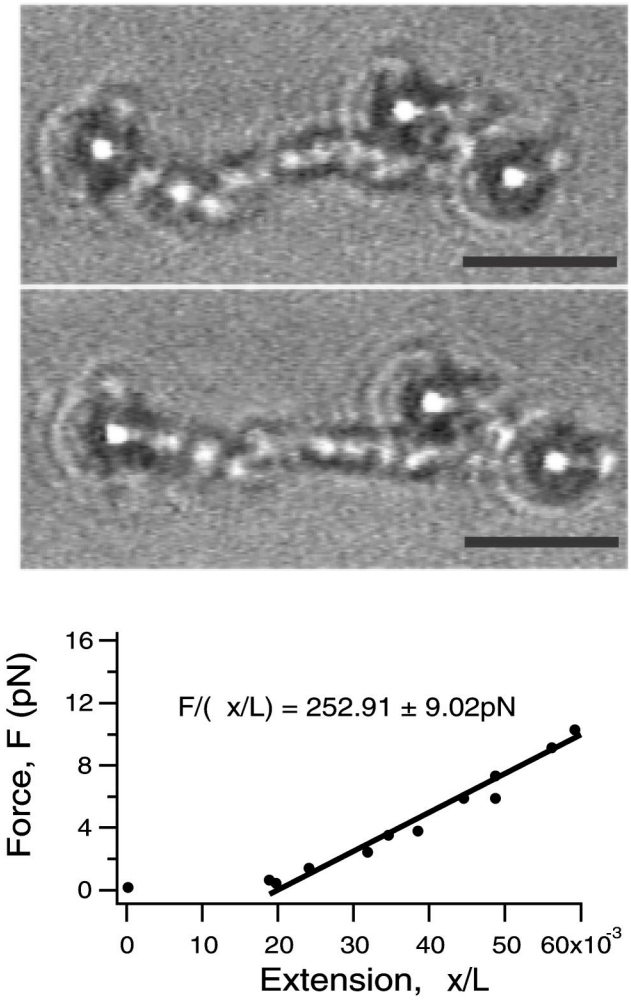

FIG. 4. Stretching experiments. Chain linked with PEG 3400 is stretched at a constant velocity of 50 μm/s. The force required to extend the chain is plotted against extension normalized by the chain length. Young's modulus is found from the slope of the linear response. Scale bar: $=5$ μm.

The stretching experiments with the PEG-linked chain show a linear response as the chain is lengthened. The stiffness of the system is determined from the modulus and converted into k_{chain} using Eq. (1). The chain stiffness is then converted into a Young modulus. For chains linked with the PEG 733, Young's modulus is $7.0\pm1.7\times10^{4}$Pa, while chains linked with the PEG 3400 has a Young modulus of $7.0\pm2.2\times10^{2}$Pa.

B. Bending experiments

In order to apply a force transverse to the long axis of the chain, the laser beams are focused onto tether handles attached to the ends of a chain. One of the beams is translated perpendicular to the long axis of the chain with motorized control of the Gimbal mirrors causing the chain to bend in the focal plane of the microscope. In Fig. 5, a chain linked with PEG 733 is bent with a force of 2.5 pN. The fit of the resulting chain shape to Eq. (5) provides the flexural rigidity. Figure 6 shows a chain linked with PEG 3400 bent with a

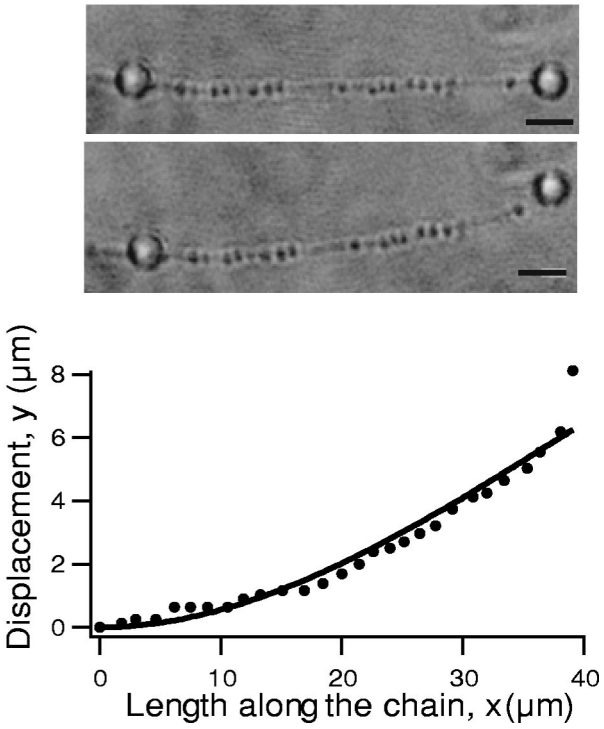

FIG. 5. Chain linked with PEG 733 is bent using optical traps at the tether handles attached to the ends. The plot of deflection vs position along the chain is fitted to Eq. (5). Scale bar: $=5$ μm.

force of 0.4 pN. A series of experiments were carried out on chains of different lengths. The average flexural rigidity values are $3.5\pm2.1\times10^{-21}$ Nm^2 for the PEG 733 linked chains and $3.2\pm1.8\times10^{-23}$ Nm^2 for the PEG 3400 linked chains.

C. Compression experiments

Similar to the bending experiments, a chain is compressed by holding one end of the chain with a tether, while the other

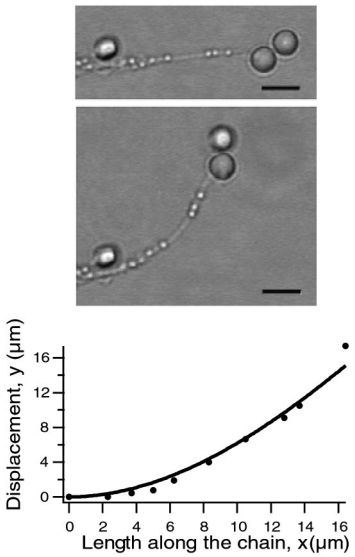

FIG. 6. Chain linked with PEG 3400 shows a greater degree of bending. Once again, the plot of deflection vs position along the chain is fitted to Eq. (5). Scale bar: $=5$ μm.

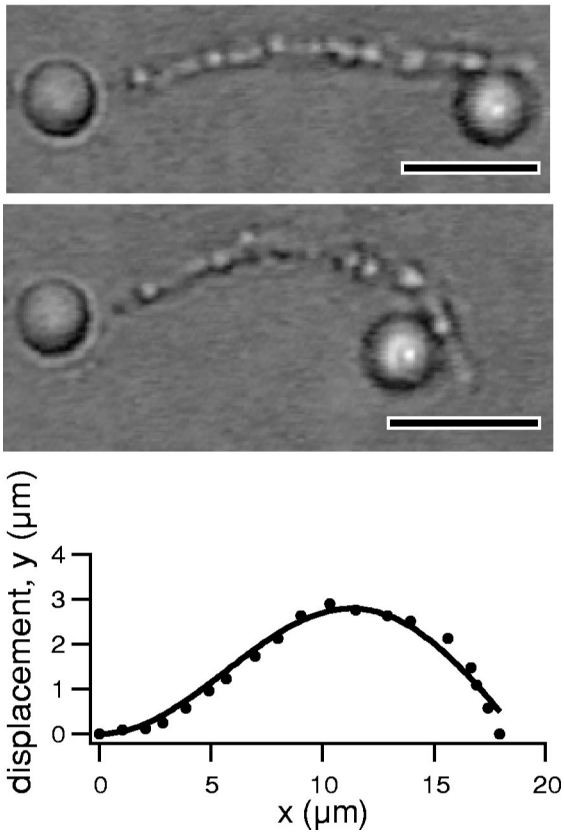

FIG. 7. Chain linked with PEG 3400 is compressed with a 2.2 pN force. The shape of the compressed chain is fitted to Eq. (8). Scale bar: $=5\ \mu$m.

end is moved with the optical tweezers parallel to the long axis of the chain such that a compressing force is applied to the chain. When the longitudinal compressing force reaches the critical force given by Euler's formula, the chain begins to bow. The compressing force used in these experiments varied from 0.3 pN to 10 pN.

The force with which a chain begins to compress can be related to the flexural rigidity; however, it is difficult to accurately observe this critical load point where a chain begins to buckle. Thus, we have chosen to analyze the resulting shape of a chain under a known compressive force to derive its flexural rigidity.

Figure 7 shows the shape of a compressed chain. Two sets of compressive experiments were done for each type of chain. In each experiment, the chain was compressed, allowed to relax, and compressed again. For the chains that are linked with the PEG 733, the average flexural rigidity is found to be $1.1\pm0.7\times10^{-21}$ Nm^2, and for the PEG 3400, the average flexural rigidity is found to be $2.2\pm1.2\times10^{-23}$ Nm^2.

D. Relaxation experiments

These experiments explore the relaxation of a chain after it is released from a constraint. As described in the bending experiments, the chain is either trapped or attached to a surface at one end of the chain and is bent at the other end of the chain by translating it perpendicular to its long axis. At a certain deflection, the end that has been translated with the optical tweezers is then released from the optical trap and the chain relaxes to its starting position. Our experiments take place at scales with typical speeds U in tens of microns per second, lengths L in tens of microns, and the kinematic viscosity ν of water of $10^6\ \mu$m^2/s. Therfore the Reynolds number of our system is $UL/\nu\sim10^{-4}$, so both the deformation and relaxation occurs at speeds where inertial forces are negligible.

The chains used in these experiments varied in length between 20–50 μm. As Fig. 8(a) shows, the PEG 733 chain relaxation from a bent state is well described by a fit to Eq. (13). This indicates that the relaxation is due to elastic forces balancing the drag force of the chain on the buffer. Figure 8(b) shows data acquired from a chain linked with PEG 3400. The PEG 733 chain is 50 μm in length and has been deflected 4.8 μm with the use of the optical tweezers, while the data shown for PEG 3400 chain correspond to a 24-μm chain that has been deflected by 7.8 μm. The exponential fits are displayed on each plot. The flexural rigidities found from Eq. (14) for these chains are $1.2\pm0.2\times10^{-21}$ Nm^2 and $2.5\pm0.3\times10^{-23}$ Nm^2 for the PEG 733 and PEG 3400 chains, respectively.

E. Glutaraldehyde-linked chains

The stiffness of the glutaraldehyde-linked chains was too high to allow measurable changes in chain shape due to stretching or compression; however, these chains do have a bending flexibility associated with them. Thus, we focused on the bending properties of these chains. Figure 9 shows a bending experiment involving a glutaraldehyde-linked chain. From the plot of the bending shape, the equation for an elastic rod does not fit the data; however, we are able to place a bound on the stiffness from the value derived from the fit: $EI>5.5\times10^{-20}$ Nm^2.

IV. DISCUSSION

We have shown that magnetoresponsive chains can be synthesized with varying degrees of flexibility. The addition of biotinylated polymer molecules to streptavidin paramagnetic particles that are aligned in an external magnetic field leads to the formation of permanently linked paramagnetic chains. In the absence of a magnetic field, these chains fluctuate like an elastic filament. Upon application of a magnetic field, they rigidify and orient in the field direction. The removal of the applied magnetic field removes the magnetic moments in the particles, and the chain becomes flexible again.

By micromanipulation with optical traps we can perform studies of chain elongation, compression, and bending. We have applied elastic models to quantify the effect of different linker lengths on the mechanical properties of the chains. Table I gives a comparison of the various elasticity measurements. The variability from one chain to another leads to differences in the absolute numbers for the flexural rigidity. The models we use assume a uniform bending moment across the length of the chain. This is not always the case for

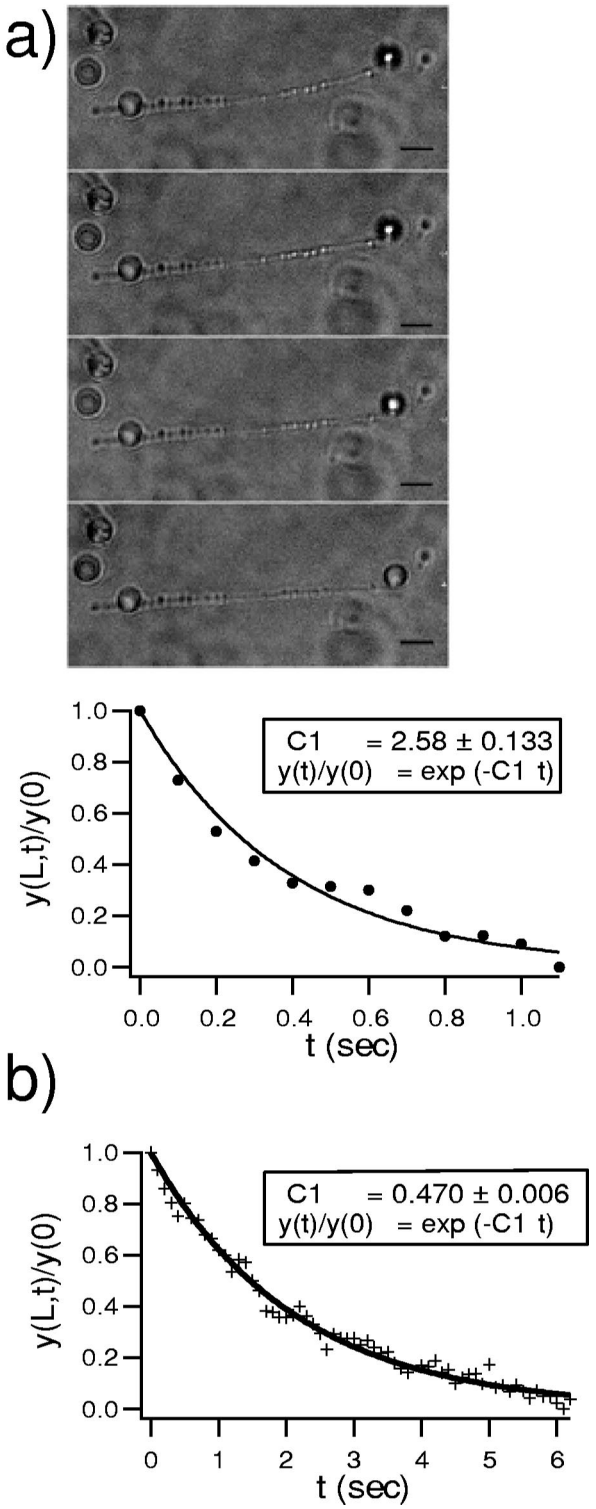

FIG. 8. Relaxation experiment. (a) Scale bar: $=5\ \mu$m. A bent chain linked with PEG 733 is released by removing the optical trap, and the chain relaxes to its starting position. The movement of the free end is fit to Eq. (13). (b) Fit of Eq. (13) to the position of free end of the chain linked with PEG 3400.

these PEG-linked chains; corrugations in the chains and inhomogeneous linkages between the particles result in changes in the elasticity along the length of a chain. Thus, there are large error limits in the flexural rigidities. We consistently find that chains linked with PEG 3400 are more flexible than chains linked with PEG 733. This indicates that the chain rigidity can be tuned by adjusting the length of the PEG chain used between the biotin linkers.

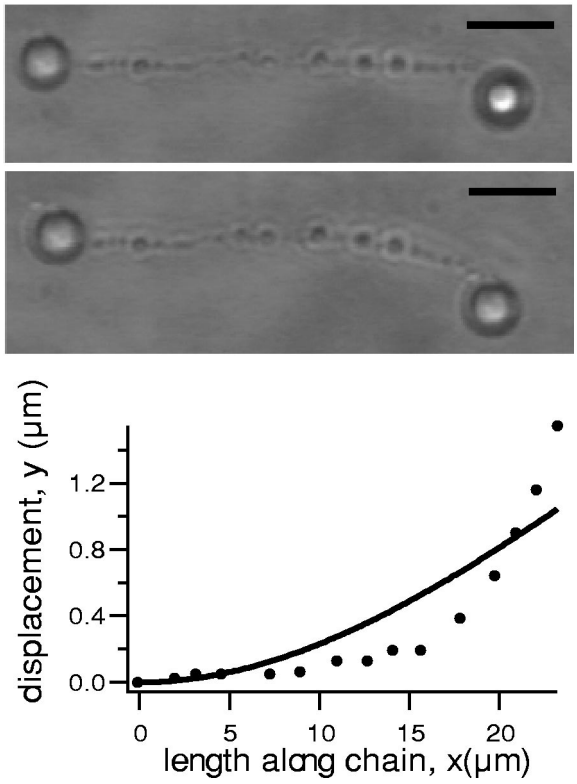

FIG. 9. Bending a chain linked with glutaraldehyde. A 25.7-μm-long chain is bent by applying a force of 11.3 pN to one end of the chain using optical tweezers. A plot of the change in shape of the chain is shown. Scale bar: $=5\ \mu$m.

The results of our optical trapping experiments show that paramagnetic particles that have been linked with PEG are Hookean for small deformations. The simplest way to imagine this to occur is to consider the geometric constraints of this system. Given the large number of streptavidin molecules per particle, there should be many attachment points between neighboring particles. Once multiple biotin linkages are made between adjacent particles, the movement of each particle becomes coupled to its neighbor. Any force along the chain becomes uniformly distributed along the length of the chain. In essence, the chain is made up of beads closely coupled by linear springs.

The average Young's moduli measured from the stretch-

TABLE I. Summary of micromanipulation results for both PEG 733 and PEG 3400 linked chains.

Experiment	PEG 733	PEG 3400
Stretching	$E=7.0\times10^{4}$ Pa	$E=7.0\times10^{2}$ Pa
Bending	$EI=3.5\times10^{-21}$ Nm^2	$EI=3.2\times10^{-23}$ Nm^2
Compression	$EI=1.1\times10^{-21}$ Nm^2	$EI=2.2\times10^{-23}$ Nm^2
Relaxation	$EI=1.2\times10^{-21}$ Nm^2	$EI=2.5\times10^{-23}$ Nm^2

ing experiments are $\sim 7\times 10^4$ Pa for the PEG 733 and $\sim 7\times 10^2$ Pa for the PEG 3400, and are much lower than that found for microtubules that have a modulus near 10^9 Pa or polymer gels that usually have moduli of 10^3–10^4 Pa. One explanation for the low modulus is that the cross-sectional area of the chain is not accurately described by the particle diameter. Though the linker itself may have a large stretching modulus, the tension applied to the chain is distributed among the linkers. A useful experiment would explore the force required to break the chain. Unfortunately, our optical traps do not have the capability to reach the ~ 257 pN [23] unbinding force between the streptavidin-biotin bond. Knowing the force needed to break the chain, we could estimate the number of linkers between each particle and estimate the cross-sectional area of the linker connectors.

We can relate the stretching and bending experiments by making the approximation that the chain is an isotropic rod with a moment of inertia $I=2\times 10^{-26}$ m^4. By multiplying by I, we can derive the flexural rigidity from the Young's modulus found from the stretching experiments: $EI \sim 10^{-21}$ Nm^2 for the PEG 733 and $\sim 10^{-23}$ Nm^2 for the PEG 3400. These calculated values of EI correspond fairly well to those found from the other micromanipulation experiments.

It is important to note that we have seen chains with defect points that are not uniformly attached as shown in Fig. 10. Possible explanations for the formation of these defects may be the incorporation of particles with poorly distributed magnetite within the latex particle. The dipole of such a particle may aggregate onto a chain with poor alignment relative to the applied field. The surface of some particles may also have poor surface coverage of streptavidin. Additionally, by increasing the temperature of the linking reaction increases the thermal agitation of the chains. This may cause corrugation in the chains while they are aligned in a magnetic field. For this reason, chains linked with PEG 3400 are more likely to have defects. These defects along the chain introduce points with different bending moments. The cross section of the chain is no longer homogeneous over its length and the evaluation of the bending energy would be better done using a bead-bead model currently being evaluated.

In summary, we have synthesized paramagnetic chains by using functionalized paramagnetic particles cross linked with a PEG spacer molecule. Paramagnetic chains have the unique ability to change stiffness with the application of an external magnetic field. Additionally, the spacer molecule allows us to selectively tailor the flexibility of chain in the absence of an external magnetic field. By changing the length of the PEG molecule, the flexibility of the chain can be adjusted. This ability to selectively choose the flexibility of the chain by both the application of an external magnetic field and the crosslinking agent makes for unique structures.

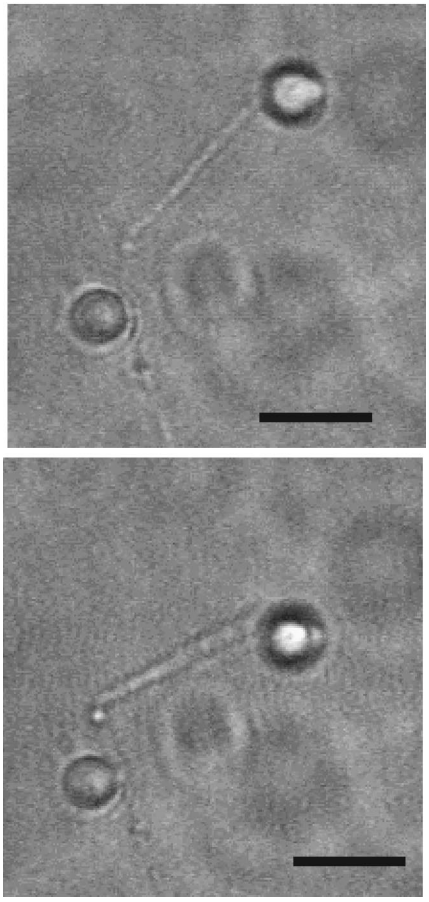

FIG. 10. Chain linked with PEG 733 without a uniform bending moment. The chain kinks as it bends. Scale bar: $=5$ μm.

We characterize the flexibility of the chain by stretching, compressing, and bending the chain with the use of optical tweezers. This information is important for the understanding of the stability of the chain under various forces in order to create useful devices. We find the flexural rigidity to be on the order of $\sim 10^{-21}$ Nm^2 for chains linked with a PEG with a molecular weight of 733. For the chains linked with a PEG with a molecular weight of 3400, we find the flexural rigidity to be on the order of $\sim 10^{-23}$ Nm^2.

ACKNOWLEDGMENT

This work was supported by the National Science Foundation, Grant No. CTS-9980860.

[1] M. Takayasu, D.R. Kelland, and J.V. Minervini, IEEE Trans. Appl. Supercond. **10**, 927 (2000).
[2] M.A. Hayes, N.A. Polson, and A.A. Garcia, Langmuir **17**, 2866 (2001).
[3] P.S. Doyle *et al.*, Science **295**, 2237 (2002).
[4] E.M. Furst *et al.*, Langmuir **14**, 7334 (1998).
[5] D.G. Grier, Curr. Opin. Colloid Interface Sci. **2**, 264 (1997).
[6] M. Kurachi, M. Hoshi, and H. Tashiro, Cell Motil. Cytoskeleton **30**, 221 (1995).
[7] H. Felgner, R. Frank, and M. Schliwa, J. Cell. Sci. **109**, 509 (1996).
[8] D. Riveline *et al.*, Biophys. J. **74**, A25 (1998).

[9] A. Chikot and P. Stayton, J. Am. Chem. Soc. **117**, 10 622 (1995).
[10] N. Green, Adv. Protein Chem. **29**, 85 (1975).
[11] L. Dorgan *et al.*, J. Magn. Magn. Mater. **194**, 69 (1999).
[12] E.M. Furst and A.P. Gast, Phys. Rev. Lett. **82**, 4130 (1999).
[13] A.D. Mehta, J.T. Finer, and J.A. Spudich, Methods Enzymol. **298**, 436 (1998).
[14] K. Visscher and S.M. Block, Methods Enzymol. **298**, 460 (1998).
[15] C. Veigel *et al.*, Biophys. J. **75**, 1424 (1998)
[16] D. Dupuis *et al.*, J. Muscle Res. Cell Motil. **18**, 17 (1997).
[17] L.D. Landau and E.M. Lifshitz, *Theory of Elasticity* (Pergamon Press, Oxford, 1986).
[18] J.M. Gere and S.P. Timoshenko, *Mechanics of Materials* (PWS, Boston, 1997).
[19] F. Gittes *et al.*, Biophys. J. **70**, 418 (1996).
[20] R. Cox, J. Fluid Mech. **44**, 791 (1970).
[21] F. Gittes *et al.*, J. Cell Biol. **120**, 923 (1993).
[22] C.H. Wiggins *et al.*, Biophys. J. **74**, 1043 (1998).
[23] V.T. Moy, E.L. Florin, and H.E. Gaub, Science **266**, 257 (1994).